Biologically inspired design of feedback control systems implemented using DNA strand displacement reactions

Foo, M., Sawlekar, R., Kulkarni, V. & Bates, D.

DOI 10.1109/EMBC.2016.7590983

Publisher: IEEE

Biologically inspired design of feedback control systems implemented using DNA strand displacement reactions

Mathias Foo, Rucha Sawlekar, Vishwesh V. Kulkarni and Declan G. Bates*

July 20, 2018

Abstract

The use of abstract chemical reaction networks (CRNs) as a modelling and design framework for the implementation of computing and control circuits using enzyme-free, entropy driven DNA strand displacement (DSD) reactions is starting to garner widespread attention in the area of synthetic biology. Previous work in this area has demonstrated the theoretical plausibility of using this approach to design biomolecular feedback control systems based on classical proportional-integral (PI) controllers, which may be constructed from CRNs implementing gain, summation and integrator operators. Here, we propose an alternative design approach that utilises the abstract chemical reactions involved in cellular signalling cycles to implement a biomolecular controller — termed a signalling-cycle (SC) controller. We compare the performance of the PI and SC controllers in closed-loop with a nonlinear second-order chemical process. Our results show that the SC controller outperforms the PI controller in terms of both performance and robustness, and also requires fewer abstract chemical reactions to implement, highlighting its potential usefulness in the construction of biomolecular control circuits.

1 INTRODUCTION

An emerging design framework that uses abstract chemical reaction networks (CRNs) in the implementation of enzyme-free, entropy driven DNA reactions has recently attracted much attention in the Synthetic Biology community following a number of successful studies [1]-[3]. The basic idea underlying this approach is to design biomolecular circuitry using abstract chemical reactions as a programming language. The designed biomolecular circuity can then be implemented directly in DNA utilising the DNA strand displacement (DSD) method [4]. Through the well-known Watson-Crick base-pairing mechanism (i.e. adenine-thymine and guanine-cytosine), the selection

*M. Foo, R. Sawlekar, V.V. Kulkarni and D.G. Bates are with Warwick Integrative Synthetic Biology Centre, School of Engineering, University of Warwick, Coventry, CV4 7AL, United Kingdom. M.Foo@warwick.ac.uk, R.Sawlekar@warwick.ac.uk, V.Kulkarni@warwick.ac.uk, D.Bates@warwick.ac.uk

of appropriate DNA sequences allows precise control over the dynamics of the implemented DNA reactions, thus facilitating a precise molecular programming of the desired function, operator or circuit. Sophisticated CAD tools are also now becoming available to facilitate the design of synthetic circuits using this approach [5]. Examples of complex biomolecular circuits successfully designed and implemented through this approach include predator-prey dynamics [6], oscillators [7], and both linear and nonlinear feedback controllers [3], [8], [9].

In [8] and [3], a classical proportional-integral (PI) controller was successfully designed using the above framework to control a biomolecular process. However, one issue that could potentially disrupt the transition from theoretical design to wet-lab implementation for such controllers is the large number of abstract chemical reactions that are required. Thus, alternative design approaches that require fewer abstract chemical reactions would be attractive from a practical point of view. In addition, little attention has so far been paid to the effect of uncertainties arising from the experimental implementation of these circuits on their functionality.

Cellular signalling cycles are ubiquitous motifs in biological systems that are implemented via a concise set of chemical reactions. Recent work on the dynamics of cellular signalling cycles [10] has revealed that they are capable of producing several distinct behaviours in terms of their input-output signal mapping that could potentially be exploited for the design of biomolecular controllers. In this paper, we show how such a signalling-cycle (SC) controller can reproduce the input-output signal mapping of a classical PI controller, while requiring smaller numbers of abstract chemical reactions to implement. We employ Monte Carlo simulation to investigate the effect of uncertainty in the reaction rates of the underlying CRNs on the stability and performance properties of both biomolecular controllers, and demonstrate that the SC controller has significantly better performance and robustness properties.

The paper is organised as follows: Section 2 describes the abstract chemical reactions used in the design of the various control systems considered, while in Section 3, we analyse the performance and robustness properties of the PI and SC feedback controllers when implemented in closed-loop with a second order nonlinear biomolecular process. Some conclusions are presented in Section 4.

2 CONTROLLER AND PROCESS DESCRIPTION

The block diagram configuration of the biomolecular feedback control system is shown in Fig. 1. In the description of the controllers and process below, we follow the variables shown in Fig. 1 closely.

2.1 PI controller

We first begin with the description of the classical PI controller designed according to the methodology of [8]. Each of the components of the feedback system can be described using abstract chemical reactions, which can then be implemented directly in DNA. As biomolecular concentrations can only take non-negative value, following the same approach as [8], the chemical species, x is split into x^+ (positive component)

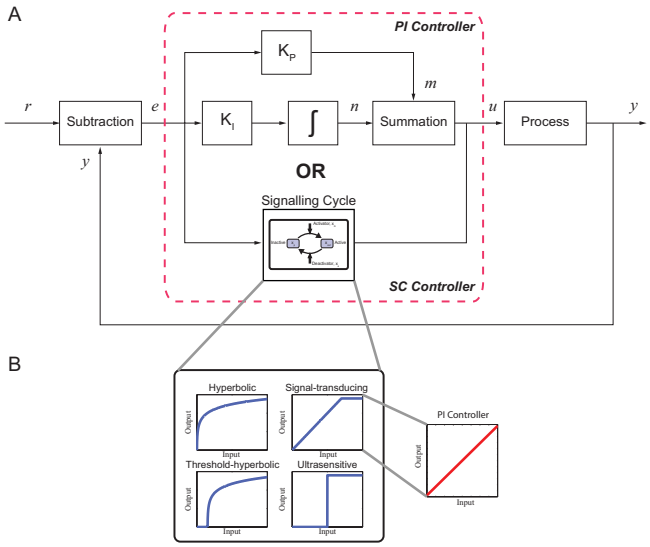

Figure 1: (A) Block diagram configuration of the biomolecular feedback control system. (B) Four different mappings of input-output signals of signalling cycle [10]. The signal-transducing mapping resembles the mapping of a PI controller.

and x^- (negative component), where $x = x^+ - x^-$ and these complementary positive and negative components annihilate each other with reaction rate, η (see below). Also, the notation $x^\pm \to x^\pm + y^\pm$ representing $x^+ \to x^+ + y^+$ and $x^- \to x^- + y^-$ is used throughout this paper. As shown in Fig. 1, the PI controller is made up of three sub-modules: an integrator, a proportional gain and a summation junction. Together these sub-modules require a total of 15 abstract chemical reactions to implement, as follows:

[Integrator:] $e^\pm \xrightarrow{K_I} e^\pm + n^\pm$ and $n^+ + n^- \xrightarrow{\eta} \emptyset$, where K_I is the integral gain of the PI controller and η is the annihilation rate.

[Proportional gain:] $e^\pm \xrightarrow{\gamma_K K_P} e^\pm + m^\pm$, $m^\pm \xrightarrow{\gamma_K} \emptyset$ and $m^+ + m^- \xrightarrow{\eta} \emptyset$, where K_P is the proportional gain of the PI controller, γ_K is the gain reaction rate.

[Summation junction:] $m^\pm \xrightarrow{\gamma_{Sm}} m^\pm + u^\pm$, $n^\pm \xrightarrow{\gamma_{Sm}} n^\pm + u^\pm$, $u^\pm \xrightarrow{\gamma_{Sm}} \emptyset$, and $u^+ + u^- \xrightarrow{\eta} \emptyset$, where γ_{Sm} is the summation reaction rate.

The tuning of this PI controller involves adjusting K_P, K_I and the reaction rates γ_K and γ_{Sm}.

2.2 SC controller

The abstract chemical reactions involved in cell signalling cycles are given by $x_p^\pm + e^\pm \xrightarrow{k_{b1}} x_{C1}^\pm$, $x_{C1}^\pm \xrightarrow{k_{b2}} u^\pm + e^\pm$, $u^\pm + x_e^\pm \xrightarrow{k_{b3}} x_{C2}^\pm$, $x_{C2}^\pm \xrightarrow{k_{b4}} x_p^\pm + x_e^\pm$, $x_p^+ + x_p^- \xrightarrow{\eta} \emptyset$, $u^+ + u^- \xrightarrow{\eta} \emptyset$, $x_{C1}^+ + x_{C1}^- \xrightarrow{\eta} \emptyset$ and $x_{C2}^+ + x_{C2}^- \xrightarrow{\eta} \emptyset$, where x_p, x_e, x_{C1} and x_{C2} are intermediate species, k_{b1} and k_{b3} are the binding rates and k_{b2} and k_{b4} are the catalytic rates. The operation of the signalling cycle can be explained as follows. $x_p^\pm$ represents the inactive

component, which gets associated with $e^{\pm}$ to form the intermediate species $x_{C1}^{\pm}$ with reaction rate k_{b1}. $x_{C1}^{\pm}$ then produces $u^{\pm}$ and the unused $e^{\pm}$ with reaction rate k_{b2}. The reverse cycle involves $u^{\pm}$ getting associated with $x_e^{\pm}$ to form intermediate species, $x_{C2}^{\pm}$, and $x_{C2}^{\pm}$ then produces back $x_p^{\pm}$ and $x_e^{\pm}$ at the rate k_{b3} and k_{b4} respectively. As shown in [10], by adjusting the reaction rates k_{b1}-k_{b4}, we can obtain four qualitatively different mapping regimes, namely hyperbolic, signal-transducing, threshold-hyperbolic and ultrasentitive [10] between the cycle's input and output signals, which we exploit in order to design our SC controller. We observe that the signal-transducing mapping regime closely resembles the input-output signal mapping of a PI Controller (see Fig. 1(B)). In view of this, we chose the SC controller's reaction rates such that it reproduces this signal-transducing mapping regime. Note that the SC controller requires 12 reactions to implement, 3 fewer than the PI controller.

2.3 Nonlinear process, closed-loop system and ODE approximations

The process that we want to control is a second order nonlinear process whose abstract chemical reactions can be described by $u^{\pm} + p^{\pm} \xrightarrow{k_{r1}} q^{\pm}$, $q^{\pm} \xrightarrow{k_{r2}} y^{\pm} + p^{\pm}$, $y^{\pm} \xrightarrow{k_{r3}} \emptyset$ and $y^{+} + y^{-} \xrightarrow{\eta} \emptyset$, where p and q are intermediate species involved in the second order process reaction. k_{r1}, k_{r2} and k_{r3} are respectively the binding, catalytic and degradation rates of the process.

In a closed-loop system, we need to compute $e := r - y$, thus requiring a subtraction operation, whose abstract chemical reactions are given as follows: $r^{\pm} \xrightarrow{\gamma_{Sb}} r^{\pm} + e^{\pm}$, $y^{\pm} \xrightarrow{\gamma_{Sb}} y^{\pm} + e^{\mp}$, $e^{\pm} \xrightarrow{\gamma_{Sb}} \emptyset$ and $e^{+} + e^{-} \xrightarrow{\eta} \emptyset$, where γ_{Sb} is the subtraction reaction rate.

Using generalised mass-action kinetics, all of the abstract chemical reactions mentioned above can be approximated by Ordinary Differential Equations (ODE) (e.g. [11]), which we use for the purposes of simulation and analysis throughout the rest of the paper. The respective ODE's for the subtraction block, PI controller, SC controller and nonlinear process are given below:

Subtraction: $\frac{de}{dt} = \gamma_{Sb}(r - y - e)$.

PI controller: $\frac{dn}{dt} = K_I e$, $\frac{dm}{dt} = \gamma_K(K_P e - m)$ and $\frac{du}{dt} = \gamma_{Sm}(m + n - u)$.

SC controller: $\frac{du}{dt} = k_{b2}x_{C1} - k_{b3}ux_e$, $\frac{dx_{C1}}{dt} = k_{b1}e - k_{b2}x_{C1}$ and $\frac{dx_{C2}}{dt} = k_{b3}ux_e - k_{b4}x_{C2}$.

Nonlinear process: $\frac{dq}{dt} = k_{r1}up - k_{r2}q$ and $\frac{dy}{dt} = k_{r2}q - k_{r3}y$.

Note that the formulation of the subtraction, gain and summation operators used in the PI controller requires identical reaction rates to be used in their sets of abstract chemical reactions. While imposing this requirement is necessary from a theoretical standpoint according to the theory in [8], implementing this requirement in an experimental setting is unlikely to be feasible, as experimental biologists are rarely able to specify the reaction rates of chemical reactions exactly. Additionally, in practice, as highlighted in [8], unregulated chemical devices or leaky expressions could potentially affect production and degradation rates and subsequently alter the behaviour of the designed component, e.g. an integrator operator could be turned into a gain operator when the rates becomes sufficiently large. To fully investigate these issues, we perform a for-

mal robustness analysis of both controllers, focussed on the effect of uncertainties in the implemented reaction rates on the closed-loop stability and performance properties of the designed feedback system.

3 RESULTS AND DISCUSSIONS

To analyse the performance and robustness of the closed-loop responses achieved by the feedback controllers with the nonlinear process, step response tests and Monte Carlo simulations are performed, respectively. For the Monte Carlo simulations, all the parameters are randomly drawn from a uniform distribution. The numbers of Monte Carlo simulations required to achieve various levels of estimation uncertainty with known probability were calculated using the well-known Chernoff bound [12]. Following the guidelines provided in [13], an accuracy level of 0.05 and a confidence level of 99% were chosen for the Monte Carlo simulation analysis, which requires a total number of 1060 simulations [12], [14]. To investigate the effect of different levels of uncertainty we vary the parameters within ranges of 20%, 50% and 100% around their nominal values. Mathematically, we have $p(1+\Delta P(x))$, where $p \in \{\gamma_{Sb1}, \gamma_{Sb2}, \gamma_{Sb3}, \gamma_{K1}, \gamma_{K2}, \gamma_{Sm1}, \gamma_{Sm2}, \gamma_{Sm3}, K_I, K_P, k_{r1}, k_{r2}, k_{r3}\}$, $P(x)$ is the probability distribution and $\Delta \in \{0.2, 0.5, 1.0\}$. Note that we split reaction rates γ_{Sb}, γ_K and γ_{Sm} according to the number of chemical reactions in which they are involved.

In our simulations, a step change in the concentration of the reference species, r from 0 M to 4 M occurs at time 0 s and the purpose of the controller is to ensure that the process output reaches this new desired concentration. As quantitative measures of the control system performance, the step response characteristics, which comprise rise time, t_r, settling time, t_s, percentage of overshoot, M_{OV} and steady state error, e_{ss} are used (see e.g. [15]). For good closed-loop performance, it is desirable to achieve a small t_r, t_s and M_{OV} as well as having $e_{ss} = 0$. As a benchmark for comparison, we first calculate the step response characteristics without parameter uncertainty. Hereafter, we refer to these as the set of results for the *nominal system*. The parameters for the nominal system in the required abstract chemical reactions are: Process: k_{r1} = 0.00005 /M/s, k_{r2} = 1.6 /s, k_{r3} = 0.0008 /s, with the total concentration constrained so that $p+q$ = 5.5 M and PI controller: γ_{Sb1}, γ_{Sb2}, γ_{Sb3}, γ_{Sm1}, γ_{Sm2}, γ_{Sm3}, γ_{K1}, γ_{K2} = 0.0004 /s, K_P = 1 and K_I = 0.0003 and SC controller: k_{b1}, k_{b3} = 0.00004 /M/s, k_{b2}, k_{b4} = 50 /s, $x_p + u + x_{C1} + x_{C2}$ = 16 M and $x_e + x_{C2}$ = 0.0033 M. The step response characteristics for both the nominal systems are tabulated in Tables 1 and 2. For each of the analysed uncertainty sets, the worst-case values of each of the step response characteristics and its associated[1] parameters are shown. For illustration, the step responses depicting the nominal and worst cases of each step response characteristic with $\Delta \in \{0.2, 0.5, 1.0\}$ are shown in Figs. 2 and 3 for PI and SC controllers respectively.

The performance of the two nominal closed-loop systems are rather similar, which reflects the fact that the SC controller was designed to reproduce the input-output mapping of the original PI controller. Interestingly, however, we can clearly see a signif-

[1]A range of parameters is given here as the associated parameter to the worst-case for each of the step characteristic is different. For example, the parameters yielding the worst t_r may not yield the worst t_s, M_{OV} and e_{ss} and vice versa.

Characteristics	Nominal	$\Delta = 0.2$	$\Delta = 0.5$	$\Delta = 1.0$
t_r (s)	10,594	24,203	37,977	Unstable
t_s (s)	34,728	49,125	92,122	Unstable
M_{OV} (%)	0.00	19.22	58.3	Unstable
e_{ss} (M)	0.00	0.79	1.87	Unstable
Parameters	**Nominal**	**$\Delta = 0.2$**	**$\Delta = 0.5$**	**$\Delta = 1.0$**
γ_{Sb1} (/s) [10^{-3}]	0.400	0.416-0.480	0.455-0.600	0.409-0.774
γ_{Sb2} (/s) [10^{-3}]	0.400	0.400-0.405	0.409-0.580	0.588-0.763
γ_{Sb3} (/s) [10^{-3}]	0.400	0.410-0.478	0.414-0.591	0.404-0.514
K_I [10^{-3}]	0.300	0.304-0.352	0.369-0.448	0.501-0.591
K_P	1.000	1.098-1.192	1.401-1.453	1.345-1.880
γ_{K1} (/s) [10^{-3}]	0.400	0.426-0.468	0.481-0.588	0.616-0.780
γ_{K2} (/s) [10^{-3}]	0.400	0.401-0.470	0.534-0.591	0.430-0.783
γ_{Sm1} (/s) [10^{-3}]	0.400	0.400-0.460	0.413-0.545	0.577-0.726
γ_{Sm2} (/s) [10^{-3}]	0.400	0.409-0.468	0.419-0.582	0.429-0.746
γ_{Sm3} (/s) [10^{-3}]	0.400	0.416-0.469	0.427-0.574	0.426-0.520
k_{r1} (/M/s) [10^{-5}]	5.000	5.067-5.872	5.028-7.352	6.635-9.000
k_{r2} (/s)	1.600	1.609-1.866	1.742-2.276	1.646-2.837
k_{r2} (/s) [10^{-4}]	8.000	8.058-9.484	8.412-11.137	8.142-9.269

Table 1: Step response characteristics and worst-case parameter ranges for the nonlinear process with PI controller.

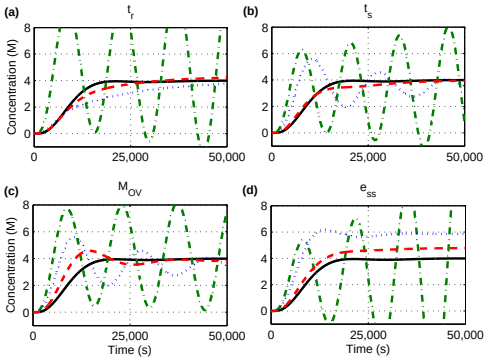

Figure 2: PI controller + nonlinear process with nominal and uncertain reaction rates: Nominal and worst cases of (a) t_r, (b) t_s, (c) M_{OV}, (d) e_{ss} with Δ = 0.2, 0.5 and 1.0. Black solid line: Nominal system. Red dashed line: worst-case response for Δ = 0.2, Blue dotted line: worst-case response for Δ = 0.5, green dash-dotted line: worst-case response for Δ = 1.0.

icantly improved robustness of the system when the SC controller is used. With the PI controller, the closed-loop system become unstable when Δ = 1, while for the SC controller the closed-loop system becomes unstable only when Δ = 1.6, showing that the SC controller is able to tolerate more than 50% more uncertainty compared to the PI controller. As shown in Fig. 4, with large Δ, we observe a significant change to the gradient of the PI controller's input-output mappings compared to SC controller. The indicates that SC controller's mapping of input-output signals are less sensitive to uncertainty thus yielding a much better robustness than the PI controller.

Note that in [9], it was shown how alternative choices of k_{b1}-k_{b4} that produce an ultrasensitive input-output mapping allowed the design of a quasi sliding mode con-

Characteristics	Nominal	$\Delta = 0.2$	$\Delta = 0.5$	$\Delta = 1.0$
t_r (s)	12,209	27,163	33,775	39,671
t_s (s)	25,791	68,902	74,841	79,385
M_{OV} (%)	0.0	9.3	26.6	51.7
e_{ss} (M)	0.00	0.73	1.77	3.67
Parameters	**Nominal**	**$\Delta = 0.2$**	**$\Delta = 0.5$**	**$\Delta = 1.0$**
γ_{sb1} (/s) [10^{-3}]	0.400	0.414-0.479	0.445-0.596	0.438-0.788
γ_{sb2} (/s) [10^{-3}]	0.400	0.401-0.479	0.409-0.520	0.408-0.736
γ_{sb3} (/s) [10^{-3}]	0.400	0.400-0.465	0.404-0.572	0.452-0.755
k_{b1} (/M/s) [10^{-4}]	0.400	0.401-0.416	0.406-0.543	0.433-0.672
k_{b2} (/s)	50.00	52.95-59.20	56.58-63.29	50.55-63.02
k_{b3} (/M/s) [10^{-4}]	0.400	0.402-0.445	0.439-0.546	0.554-0.775
k_{b4} (/s)	50.00	52.54-59.80	56.58-63.29	50.55-63.02
k_{r1} (/M/s) [10^{-5}]	5.000	5.093-5.995	5.135-7.166	6.002-8.803
k_{r2} (/s)	1.600	1.625-1.831	1.612-2.176	1.993-2.873
k_{r2} (/s) [10^{-4}]	8.000	8.088-9.289	8.022-11.019	8.019-13.465

Table 2: Step response characteristics and worst-case parameter ranges for the nonlinear process with SC controller.

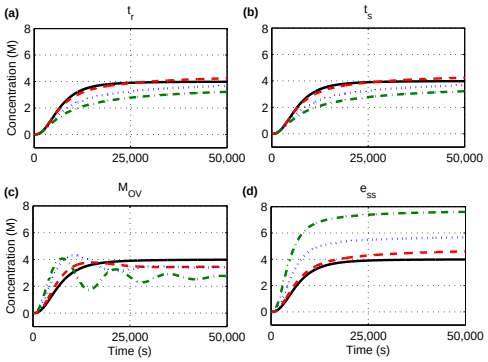

Figure 3: SC controller + nonlinear process with nominal and uncertain reaction rates: Nominal and worst cases of (a) t_r, (b) t_s, (c) M_{OV}, (d) e_{ss} with Δ = 0.2, 0.5 and 1.0. Black solid line: Nominal system. Red dashed line: worst-case response for Δ = 0.2, Blue dotted line: worst-case response for Δ = 0.5, green dash-dotted line: worst-case response for Δ = 1.0.

troller, further showcasing the versatility of this particular CRN for the purposes of control system design.

4 CONCLUSIONS

The framework of using utilising abstract chemical reaction to design embedded synthetic feedback circuits that can be implemented using enzyme-free, entropy driven DNA reactions has huge potential in the field of Synthetic Biology. Here, we analysed the performance and robustness of two biomolecular feedback control systems, a linear PI controller and a biologically inspired nonlinear SC controller. Our findings reveal that SC controller has better performance and robustness than the PI controller. Addi-

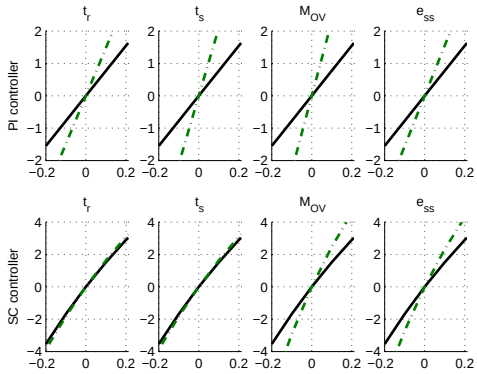

Figure 4: The mappings of input-output signals of PI controller (top row) and SC controller (bottom row). Black solid line: Nominal system. Green dash-dotted line: worst-case response for $\Delta = 1$.

tionally, the design requires lesser abstract chemical reactions. These results highlight the great potential usefulness of SC controller in the implementation of biomolecular control systems.

5 ACKNOWLEDGEMENTS

We gratefully acknowledge the financial support from EPSRC via research grant EP/M002187/1, BBSRC via research grants BB/M017982/1 and from the School of Engineering of the University of Warwick.

References

[1] G. Seelig, D. Soloveichik, D.Y. Zhang and E. Winfree, "Enzyme-free nucleic acid logic circuits", *Science*, vol. 314, no. 5805, pp. 1585-1588, 2006.

[2] L. Qian and E. Winfree, "A simple DNA gate motif for synthesizing large-scale circuits", *Journal of the Royal Society of Interface*, p.rsif20100729, 2011.

[3] B. Yordanov, J. Kim, R.L. Petersen, A. Shudy, V.V. Kulkarni and A. Philips, "Computational design of nucleic acid feedback control circuits" *ACS Synthetic Biology*, vol. 3, no. 8, pp. 600-616, 2014.

[4] D. Soloveichik, G. Seelig, and E. Winfree, "DNA as a universal substrate for chemical kinetics" *Proceedings of National Academy of Sciences, USA*, vol. 107, no. 12, pp. 5393-5398, 2010.

[5] M.R. Lakin, S. Youssef, F. Polo, S. Emmott, and A. Phillips1, "Visual DSD: a design and analysis tool for DNA strand displacement systems" *Bioinformatics*, vol. 27, no. 22, pp. 3211-3213, 2011.

[6] T. Fujii and Y. Rondelez, "Predator-prey molecular ecosystems", *ACS Nano*, vol. 7, no. 1, pp. 27-34, 2013.

[7] M. Weitz, J. Kim, K. Kapsner, E. Winfree, E. Franco and F.C. Simmel, "Diversity in the dynamical behaviour of a compartmentalized programmable biochemical oscillator", *Nature Chemistry*, vol. 6, pp. 295-302, 2014.

[8] K. Oishi and E. Klavins, "Biomolecular implementation of linear I/O systems", *IET Systems Biology*, vol.5, issue. 4, pp. 252-260, 2011.

[9] R. Sawlekar, F. Montefusco, V.V. Kulkarni and D.G. Bates, "Biomolecular implementation of a quasi sliding mode feedback controller based on DNA strand displacement reactions", *Proceedings of IEEE Engineering in Medicine and Biology Conference*, Milan, Italy, 2015.

[10] C. Gomez-Uribe, G.C. Verghese and L.A. Mirny, "Operating regimes of signaling cycles: statics, dynamics, and noise filter", *PLoS Computational Biology*, vol. 3, pp. e246, 2007.

[11] M. Feinberg, "Lectures on chemical reaction networks", *Notes of lectures given at the Mathematics Research Center, University of Wisconsin*.

[12] M. Vidyasagar, "Statistical learning theory and randomised algorithms for control", *IEEE Control Systems Technology*, vol. 18, no. 6, pp. 69-85, 1998.

[13] P.S. Williams, "A Monte Carlo dispersion analysis of the x-33 simulation software". *Proceedings of AIAA Conference on Guidance, Navigation and Control*, Montreal, Canada, 2001.

[14] P.P. Menon , I. Postlethwaite, S. Bennani, A. Marcos and D.G. Bates "Robustness analysis of a reusable launch vehicle flight control law", *Control Engineering Practice*, vol. 17, no. 7, pp. 751-765, 2009.

[15] G.F. Franklin, J.D. Powell and A. Emami-Naeini, *Feedback control of dynamic systems*, 7th Edition, Pearson, 2015.